Contents lists available at ScienceDirect

Ultrasonics - Sonochemistry

journal homepage: www.elsevier.com

Pulsed ultrasound for temperature control and clogging prevention in micro-reactors

Claire Delacour [a], Cecile Lutz [b], Simon Kuhn [a]

[a] KU Leuven, Department of Chemical Engineering, Celestijnenlaan 200F, 3001 Leuven, Belgium
[b] Service Adsorption, ARKEMA, Groupement de Recherche de Lacq, 64170 Lacq, France

ARTICLE INFO

Keywords:
Ultrasonic micro-reactor
Pulsed ultrasound
Temperature control
Clogging prevention
Effective ultrasonic treatment time

ABSTRACT

Ultrasonic micro-reactors are frequently applied to prevent micro-channel clogging in the presence of solid materials. Continuous sonication will lead to a sizeable energy input resulting in a temperature increase in the fluidic channels and concerns regarding microchannel degradation. In this paper, we investigate the application of pulsed ultrasound as a less invasive approach to prevent micro-channel clogging, while also controlling the temperature increase. The inorganic precipitation of barium sulfate particles was studied, and the impact of the effective ultrasonic treatment ratio, frequency and load power on the particle size distribution, pressure and temperature was quantified in comparison to non-sonicated experiments. The precipitation reactions were performed in a continuous reactor consisting of a micro-reactor chip attached to a Langevin-type transducer. It was found that adjusting the pulsed ultrasound conditions prevented microchannel clogging by reducing the particle size to the same magnitude as observed for continuous sonication. Furthermore, reducing the effective treatment ratio from 100 to 12.5% decreases the temperature rise from 7 to 1 °C.

1. Introduction

More than 80% of the chemical processes involve solids [1], either as reactant, catalyst or product. Different methods have been developed to increase the control of particle synthesis processes, and applying low frequency ultrasound is one of them [2]. By changing ultrasound parameters like the load power, applied frequency, contact time or reactor geometry, it was shown that ultrasound provides control on particle size distribution for both organic and inorganic particles by preventing agglomeration [3–5]. Jordens et al. [3] studied the effect of frequency and applied power on the particle size distribution and morphology of manganese carbonate. This precipitation reaction was carried out in a batch reactor attached to a Langevin-type transducer. The studied frequencies were 94, 577 and 1135 kHz. It was observed that particle size decreases when ultrasound is applied as a result of increased cavitation activity. However, the observed particle size was independent of the applied frequency. Barium sulfate precipitation has been studied by Pohl et al. [6] in two different reactors called conical and cavitation chamber reactors. Ultrasound was applied by using a 20 kHz sonotrode. Results showed that ultrasound enhances mixing and nucleation, and that the particle sizes and morphology changed with output power. Dodds et al. [7] obtained uniform distribution of particles when studying the sono-precipitation of barium sulfate. Reactions were performed in semi-batch and continuous mode reactors. A 20 kHz ultrasonic equipment was used. A monomodal and more narrow distribution was obtained under continuous sonication compared to silent conditions.

However, a major drawback of applying low frequency ultrasound and exploiting the cavitation phenomena is the increase in temperature due to the collapse of the bubbles. These collapses lead to the formation of hot spots of high temperature (>5000 K) and high pressure (>1000 atm). Such a temperature increase impacts on different scales: for chemical reactions, it is important to have an accurate temperature control, especially when working with temperature sensitive reactants, as it can impact the quality and yield of the reaction [8]. This increase in temperature can also affect the gas solubility and vapor pressure, which will reduce the cavitation activity [9,10]. Two different temperature control approaches have to be distinguished, i.e. external and internal temperature control. For the external temperature control, heating and cooling elements such as Peltier elements or air fans are usually used. The common approach to control the internal temperature of the reaction mixture is to use a circulating flow of a heat exchange fluid, where water is mainly used [3,11,12]. For instance, Dalvi and Yadav [12] used a jacketed batch reactor with an immersed ultrasonic horn for curcumin anti-solvent precipitation. John et al. developed a temperature controlled interval contact reactor [8], by combining a small-scale ultrasonic bath with an ultrasonic interval contact reactor [13,14]. In this work, we establish an ultrasound application strategy to achieve both the external and internal temperature control of the micro-fluidic device without the need for additional cooling.

https://doi.org/10.1016/j.ultsonch.2019.03.012
Received 29 November 2018; Received in revised form 5 March 2019; Accepted 9 March 2019
Available online xxx
1350-4177/

This is realized by adjusting the ultrasound contact time when using pulsed ultrasound, which alternates a time under ultrasound (t_{US}) followed by a time under silent condition (t_{silent}). Table 1 shows selected organic and inorganic particle synthesis in batch reactors under pulsed ultrasound conditions. It is observed that different definitions of the duty cycle are used.

Despite the different definitions given by the authors, pulsed ultrasound showed some advantages. First, an increase in cavitation activity is observed under pulsed ultrasound compared to continuous sonication. Ashokkumar [23] studied this phenomenon by sonoluminescence measurements. The pulsed ultrasound cycle corresponds to 4 ms under ultrasound and 12 ms under silent conditions at a frequency of 515 kHz. The cavitation activity reaches a stable plateau after 16 cycles. Ciaravino et al. [24] evaluated the effect of pulsed ultrasound on the cavitation activity by quantifying the release of iodine (Weissler reaction). A 1.06 MHz ultrasonic equipment was used at intensities of 10, 20 and 30 W/cm^2. A duty cycle of 1:1 (equal times with and without ultrasound) was used, and the results showed that the cavitation activity depends on the duty cycle, load power and frequency [2]. It has been shown that optimizing the pulsed ultrasound condition results in an increase of 6% of iodine release for intensities of 20 W/cm^2 and 30 W/cm^2 compared to continuous sonication. Then, concerning the effect of pulsed ultrasound on particles, Zhu et al. [25] produced silver nanoparticles under different shape under pulsed sonoelectrochemical conditions.

Table 1
Selected organic and inorganic particle synthesis in batch reactors under pulsed ultrasound conditions.

Research team	Process	Set-up	Ultrasound conditions
Louisnard et al. [15]	Crystallization of glycine	20 kHz ultrasonic horn immersed in a batch reactor	Duty cycle = t_{US}/t_{silent}
Gielen et al. [16]	Cooling crystallization of paracetamol	30 kHz ultrasonic horn immersed in a batch reactor	Duty cycle = $t_{US}/(t_{US} + t_{silent})$ t_{US} is kept constant at 0.2 s
Guo et al. [17]	Anti-solvent crystallization of roxithromycin	Titanium probe immersed in a batch reactor	t_{US} = 2 s t_{silent} = 5 s
Rahmani et al. [18]	Cr/clinoptilolite-ZrO2 nanocatalyst synthesis	20 kHz titanium horn in a batch reactor	t_{US} = 0.3 s t_{silent} = 0.1 s
Boffito et al. [19]	Sulphated zirconia and mixed zirconia/titania prepared by sol–gel synthesis	20 kHz ultrasonic horn in a water-jacketed reactor	Pulse ON/OFF: 0.1/0.9; 0.3/0.7; 0.5/0.5 s and continuous sonication
Jiang et al. [20]	Silver nanoparticle sonoelectrochemical synthesis	Titanium horn in a batch reactor	Sonic pulse (t_{US}) followed by a current pulse ($t_{current}$). $t_{US} = t_{current}$ = 3 s
Zhu et al. [21]	Silver nanoparticle sonoelectrochemical synthesis	Titanium horn in a batch reactor	Sonic pulse (t_{US}) followed by a current pulse ($t_{current}$). $t_{US}/t_{current}$ = 0.5 with $t_{current}$ = 0.3 s
Hass et al. [22]	Copper nanoparticles sonoelectrochemical synthesis	Ultrasonic horn in a batch reactor	Pulsation conditions are composed of current and ultrasound pulses

As summarized above, experiments under pulsed ultrasound are widely described and used under batch conditions. In this work, pulsed ultrasound conditions will be applied to the synthesis of an inorganic compound in a micro-reactor. The increasing demand for continuous manufacturing of chemicals and pharmaceuticals led to the development of micro- and milli-scale reactors due to their advantages like enhanced heat/mass transfer, safer operation, enhanced process reproducibility, and scale-up potential [26–28]. Nevertheless, despite those advantages their inability to deal with solids still remains an important issue. Applying continuous low frequency ultrasound [29–32] or high frequency ultrasound (>1MHz) [33] in continuous micro- and milli-scale reactors successfully prevents clogging. However, depending on the applied frequency, different phenomena are observed. The application of high frequency ultrasound results in acoustophoretic forces which alter the trajectory of particles without destroying aggregates. The application of low frequency ultrasound results in increased cavitation activity which promotes the breakage of agglomerates. However, the associated temperature increase and concerns regarding microchannel degradation due to the high cavitation intensity [29] always accompanied the use of low frequency ultrasound. In this paper we study the potential of applying pulsed low frequency ultrasound for clogging prevention and its effect on the particle size distribution of barium sulfate precipitates. It is observed that reducing the effective ultrasound treatment time from 100% to 12.5% per residence time is sufficient to prevent clogging, while the choice of all ultrasound parameters enables the synthesis of particles with different size distribution. Therefore, this study presents an energy efficient process for particle synthesis in micro-reactors using milder ultrasound conditions.

2. Materials and methods

2.1. Chemicals

Barium sulfate particles ($BaSO_4$) were obtained by mixing an aqueous solution of barium chloride dihydrate ($BaCl_2$, $2H_2O$, Flasher Chemical, Laboratory reagent grade, 0.043 M) with an aqueous solution of sodium sulfate (Na_2SO_4, Accros Organics, 99% purity, 0.05 M). To clean the micro-channels after the reaction, the reactor was washed with a saturated solution of sodium carbonate (Na_2CO_3, Accros Organics, 99.5% purity) and then with acetic acid (Chemlab, 99–100% purity). All solutions were prepared with deionized water.

2.2. Experimental setup

Experiments were carried out in an ultrasonic micro-reactor (USMR). The USMR consists of a micro-reactor glued to a Langevin-type transducer [34–36]. The Langevin-type transducer is designed to vibrate as a half-wavelength resonator in the longitudinal direction. The micro-reactor is made of silicon with a glass top as enclosure. The microchannel has a square cross-section of 0.6×0.6 mm^2 and its total volume is 0.513 mL. A number of holes were drilled in the glass top layer which act as reactant inlet and outlet, but also to insert a temperature probe (Omega HH374 thermocouple). A pressure sensor (Elveflow sensor reader, 15 psi) is connected to the Na_2SO_4 line. Impedance measurements were performed (Sinephase 16777 k) to determine the resonance frequencies of the USMR system. Two resonance frequencies were observed, the first at approximately 21 kHz and the second at approximately 46 kHz. The USMR is connected to a power amplifier (E&I, RF 2100L, 100 W) and a waveform generator (Keysight 33500B, series waveform). The output signal is checked with an oscilloscope (Keysight DS0X1102A, Digital Storage Oscilloscope, 70 MHz – 2 GSa/s). Syringe pumps (Harvard pump PHD) were used to deliver reactants in the reactor channel at a

total flow rate of 0.2 mL/min. The USMR arrangement and the experimental setup is depicted in Fig. 1. Fig. 1b) and c) visualize the different reactor outlets. For preliminary experiments to screen the effect of residence time under silent conditions two outlets have been used, which correspond to a reactor volume of 0.264 mL and 0.513 mL respectively. In the sonicated experiments only one outlet is used corresponding to the volume of 0.264 mL.

In addition to recording continuously pressure drop and temperature, particle size distribution offline measurements (based on volume) were done after 10, 20 and 30 min of reaction using a Laser diffractometer (Malvern, MasterSizer hydro SV). The volume of the cell is 7 mL. The cell is filled with deionized water and after initializing the system, 1 mL of sample is added. For the analysis, the values Dv(10), Dv(50) and Dv(90) corresponding to 10, 50 and 90% of the particles being below a certain size, and the width of the distribution (Dv(90) – Dv(10)) are plotted as function of the studied parameters.

Pulsed ultrasound conditions were studied to quantify the temperature increase when an entire ultrasound cycle equaling to the residence time (t_r) of 80 s is split into a time under ultrasound (t_{US}) and a time under silent conditions (t_{silent}). For these pulsed ultrasound conditions, the effective ultrasonic treatment ratio is defined as the time under ultrasound divided by the residence time:

$$\textit{Effective ultrasonic treatment ratio} = \frac{t_{US}}{t_r} \times 100, \quad \text{with } t_r = t_{US} + t_{silent}$$

This residence time has been determined during a preliminary study. In these preliminary experiments the residence time was varied from 12.5 s to 120 s under silent conditions. In this studied range the residence time of $t_r = 80$ s was identified to result in a stable particle formation over time without immediate reactor clogging. Hence, this residence time was used as reference for the sonicated experiments. There, we first studied the impact of the effective ultrasonic treatment ratio at this constant residence time. The ultrasonic irradiation is delivered in a single pulse, and the studied effective ultrasonic treatment ratios were 0, 12.5, 50 and 100%, where 0 and 100% corresponds to silent and continuous sonication conditions respectively. Secondly, the effect of delivering the same energy input spread over 2 pulses was studied. For this, the effective ultrasonic treatment ratio per residence time is fixed at 12.5%, which is either delivered as a single pulse of 10 s followed by 70 s under silent conditions, or split into two pulses of 5 s separated by a time under silent conditions of 35 s. Those sequences are repeated during 30 min, and their details are found in Table 2 and Fig. 2.

2.3. Calorimetric power measurement

Calorimetric measurements were performed to quantify the amount of ultrasound power transferred to the fluid in the microchannel. The transducer is composed of a piezoelectric material which converts electrical energy into mechanical energy, which is then converted into thermal energy. The calorimetric dissipation

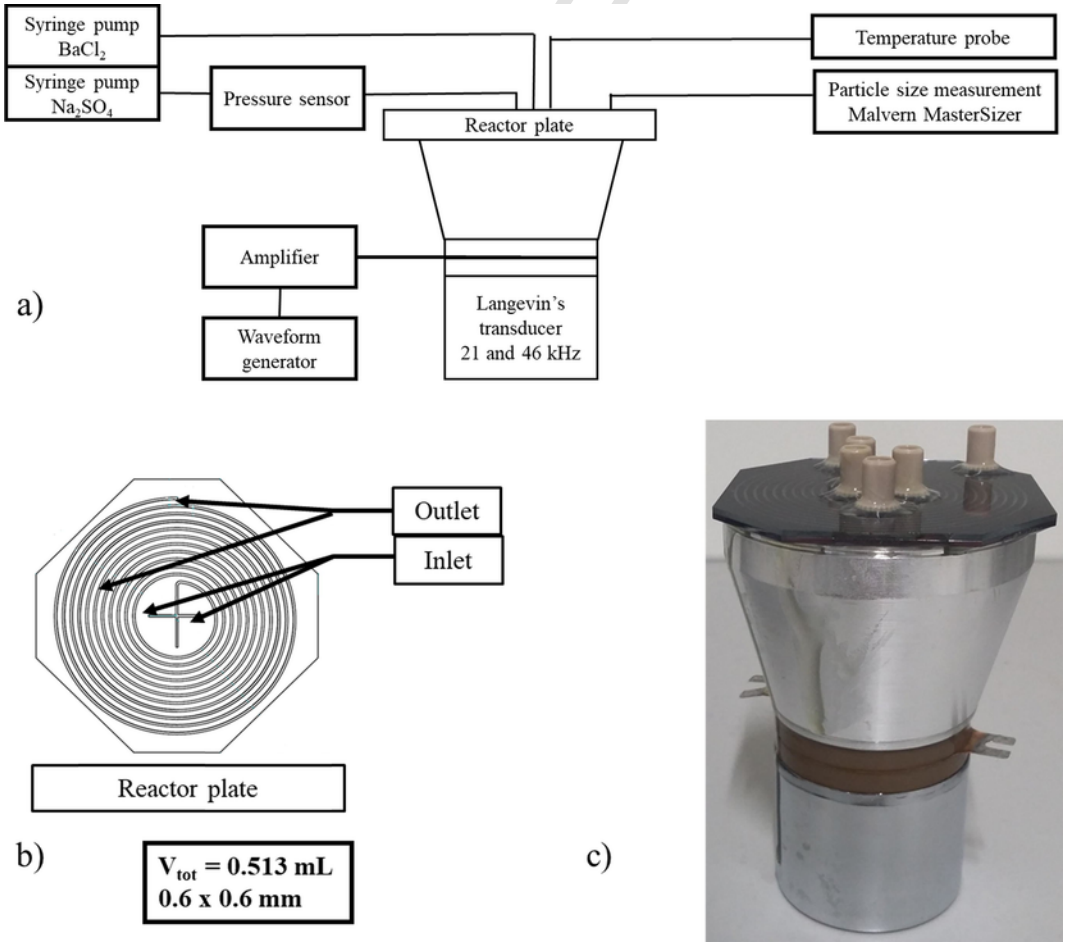

Fig. 1. a) Ultrasonic micro-reactor experimental set-up consisting of a reactor plate attached to a Langevin's type transducer. Syringe pumps are used to deliver the reactants, and a pressure and a temperature sensor is connected. b) The micro-channel consists of a square cross-section of 0.6 × 0.6 mm^2, with drilled holes for inlets and outlets. c) Photograph of the ultrasonic micro-reactor consisting of the reactor plate and a dual frequency Langevin's type transducer.

Table 2
Investigated effective ultrasound treatment ratio and operating conditions, where t_{US} corresponds to the time under ultrasound, t_{silent}, to the time under silent conditions and t_r represents the residence time in the micro-reactor which is defined by the applied flow rates.

Effective ultrasound treatment ratio (%)	t_{US} (s)	t_{silent} (s)	t_r (s)
0	0	80	80
12.5	10	70	80
12.5	2 × 5	2 × 35	80
50	40	40	80
100	80	0	80

power corresponds to the sum of (i) the energy responsible for increasing the reaction mixture temperature, (ii) the energy absorbed by the reactor wall and transducer and (iii) the energy lost to the ambient temperature [37].

However, for the calculations, the energy absorbed by the reactor wall and the transducer has been neglected as the reactor is made of low thermal conductivity materials. The energy lost to the ambient air is due to convective mode of heat transfer. Those effects have less significance at laboratory scale than at larger scale, as the volume of reactors are in the range of few mL. At larger scale, the surface in contact with air is much more important so that the convective mode of heat transfer has to be taken into account.

To quantify the calorimetric power, P_{cal}, the change of temperature ΔT was recorded for a time interval Δt corresponding to 5 reactor volumes at a flow rate of 0.2 mL/min,

$$P_{cal}(W) = mc_p \frac{'T}{'t}$$

where m is the mass of liquid irradiated by ultrasound, and c_p is the heat capacity of the fluid.

3. Results and discussions

3.1. Influence of effective ultrasonic treatment ratio

The influence of the effective ultrasonic treatment ratio on clogging prevention and on the particle size distribution is investigated first. For these experiments the frequency was set to 21 kHz at a load power of 11 W. The effective ultrasonic treatment ratio was varied between 0, 12.5, 50 and 100% (see Table 2), where 0% represents silent conditions and 100% continuous sonication. Fig. 3 depicts the influence of the effective ultrasonic treatment ratio on the resulting particles size distributions. Upon sonication (both pulsed and continuous) the mean particle size as well as the span of the size distribution decreases. Larger particle sizes are observed under silent conditions, which can be explained by the presence of agglomerates. Thus, both pulsed and continuous ultrasound minimizes particle agglomeration by reducing the contact time between particles and by breaking up agglomerates [38].

This observation is also confirmed by the narrow size distribution obtained under ultrasound. This showed that a more uniform distribution is obtained due to the increase in mixing efficiency. This effect has been observed by Pohl et al. [6] for the ultrasound precipitation of barium sulfate. It has been shown that the number of small particles increases when increasing the quality of micro-mixing. Enhanced micro-mixing quality will lead to a better distribution of the reactant along the reactor channel.

Comparing pulsed and continuous ultrasound conditions, it is observed that both the mean particle size and the span is similar for an effective ultrasonic treatment ratio of 50% and 100%, whereas a smaller mean size and span is found for 12.5%. This difference can be explained by the micro-mixing effects provided by ultrasound. Sonication will improve the mixing between the reagents, and consequently an increase in sonication time will result in an increased number concentration of small particles. This increase of concentration of small particles leads to the formation of stable aggregates due to the large adhesive interaction potential of barium sulfate particles [39,40]. This phenomenon might promote agglomeration, which il-

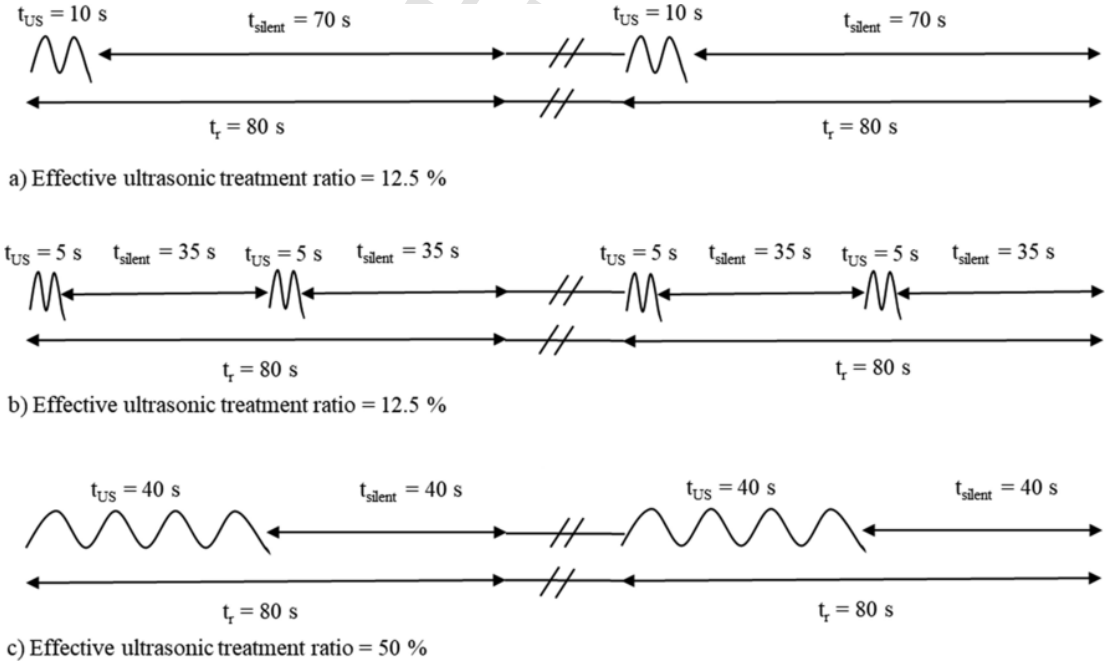

Fig. 2. Schematic of the studied pulsed ultrasound sequences. The length of each cycle corresponds to the mean residence time of 80 s.

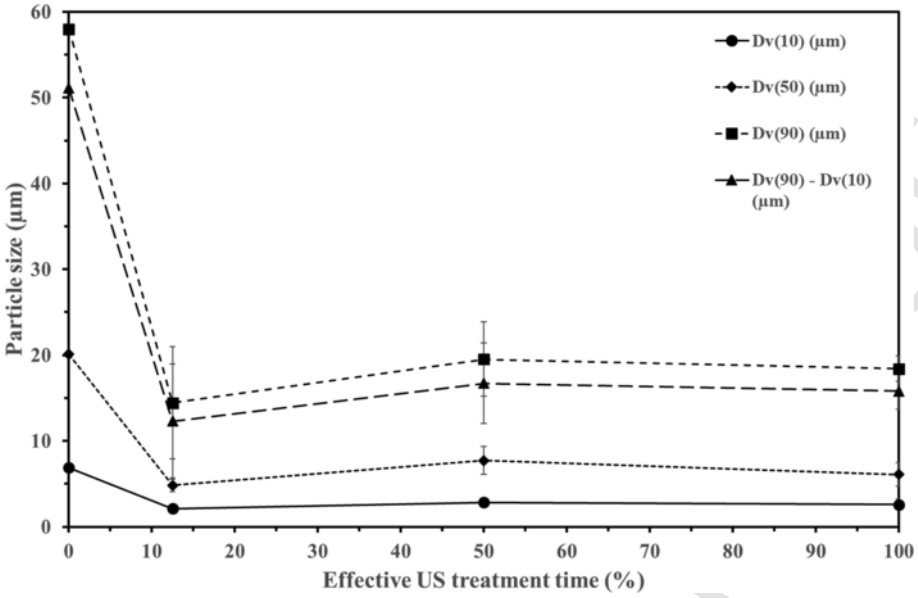

Fig. 3. Effect of the effective ultrasonic treatment ratio on the characteristics dimensions Dv(X) of the volume based PSD obtained at a flow rate of 0.2 mL/min and a concentration of 0.043 M with an applied frequency of 21 kHz and at a load power of 11 W (t_r = 80 s).

lustrates the fact that ultrasound can both promote and prevent agglomeration [41].

The pressure drop over the entire reactor was recorded for all ultrasound conditions. Under silent conditions the pressure drop is continuously increasing which leads to channel clogging after 15 min. For both pulsed and continuous sonication, no pressure increase was observed during 30 min of reaction, thus both pulsed and continuous sonication can efficiently prevent clogging. It is worth noting that applying ultrasound for only 12.5% of the total 80 s of residence time are sufficient to ensure continuous operation.

3.2. Effect of number of sonication pulses at a fixed effective ultrasonic treatment ratio

Next, the effect of the number of ultrasound application pulses at a fixed effective ultrasonic treatment ratio is investigated. For this, the studied ratio is set to 12.5% at a frequency of 21 kHz and a load power of 11 W. Two different ultrasound cycles are compared: i) the 12.5% of ultrasound irradiation will be delivered in a single pulse (labelled 1 son); ii) the 12.5% of ultrasound irradiation is delivered in two pulses of 5 s each separated by 35 s (labelled 2 son). The corresponding results are depicted in Fig. 4, and it is observed that both the Dv(10) and Dv(50) are quite similar for both conditions. However, a narrower size distribution is obtained in the case of two pulses per residence time. This more narrow distribution might be explained by an enhancement of the cavitation bubble activity as described by Gielen et al. [16]. During the time under ultrasound cavitation bubbles are formed and oscillate, and they dissolve during the silent time. Applying the second pulse shortly thereafter allows to reactivate the cavitation bubbles.

The bigger particles observed in the case of 1 son compared to 2 son can also be explained by the different growth time (equaling the

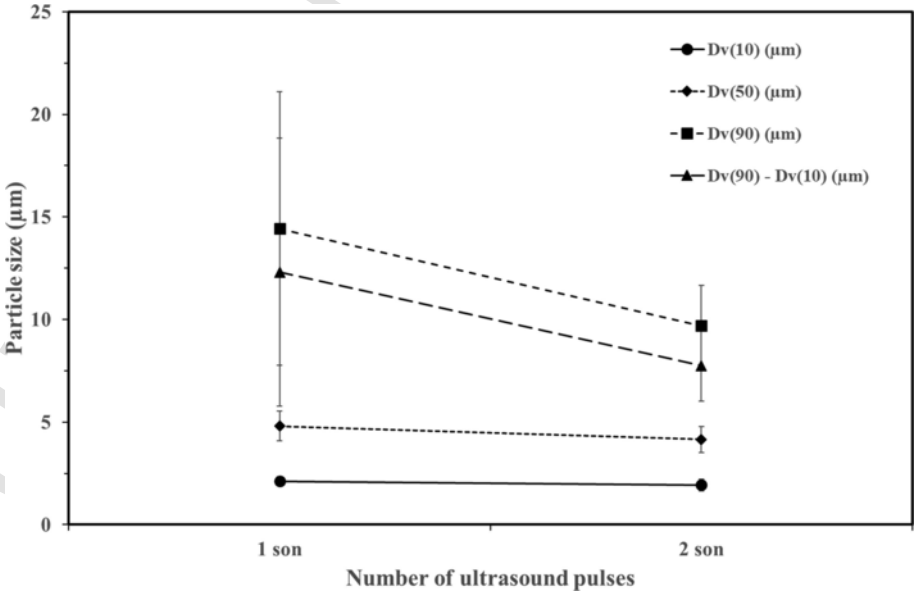

Fig. 4. Effect of the pulse number on the characteristic dimension $D_v(X)$ of the volume based PSD at a fixed effective ultrasonic treatment ratio of 12.5% obtained at a fixed flow rate of 0.2 mL/min, a concentration of 0.043 M, with an applied frequency of 21 kHz and at a load power of 11 W (t_r = 80 s).

silent time). In the case of 1 son, particles have more time to grow and to form agglomerates. This combined effect of ultrasound and growth time also causes the narrower size distribution for the 2 son case. Particle agglomerates which grow during the first silent time are again reduced by the second ultrasound pulse. Moreover, it can be noticed that the variability in the characteristic dimensions of the particle size distribution is enhanced when the effective ultrasonic treatment ratio per residence time is divided in two pulses of 5 s separated by a silent time of 35 s. This observation can be explained by the fact that the second pulse allows the sonication of particles which were not yet generated during the first pulse. This allows to increase the repeatability of operating conditions at a low effective ultrasonic treatment ratio.

Also in these experiments the pressure drop over the entire micro-reactor was recorded, and no pressure increase was observed for both conditions. Thus, both pulsed ultrasound conditions prevent micro-channel clogging.

3.3. Effect of ultrasonic parameters

The effect of both applied frequency and load power was studied at an effective ultrasonic treatment ratio of 50% per residence time. To investigate the effect of frequency the load power was fixed at 11 W and two frequencies were studied: 21 and 46 kHz. Those frequencies correspond to the resonance frequencies of the USMR. The obtained results are summarized in Table 3. The observed particle sizes are independent of the applied frequency. This observation is in line with Jordens et al. for the precipitation of manganese carbonate [3]. Lee et al. observed the same phenomenon for the anti-solvent crystallization of sodium chloride [4]. Despite the fact that the cavitation activity changes with frequency, particle sizes are independent of frequency. An explanation to this observation is that the threshold in size is achieved at the studied load power so that frequency will not impact the size distribution. This threshold effect has also been shown by Jordens et al. [3] for the precipitation of manganese carbonate. In fact, at a low intensity of 5 W/L, particle sizes increased when increasing the frequency. This phenomenon was not observed at an intensity of 49 W/L.

To study the effect of the load power the frequency was fixed at 21 kHz and two load powers were studied: 11 W and 22 W. The resulting particle sizes are listed in Table 4, where a size decrease for all size classes with increasing power is observed. This is due to the increase in cavitation activity, which leads to the formation of more cavitation bubbles, and subsequent break-up of particle agglomerates.

The same effect of load power and frequency on particle size distributions were observed under pulsed ultrasound conditions compared with continuous sonication [3–5].

Table 3
Effect of frequency on characteristic dimensions $D_v(X)$ of the volume based PSD obtained at an effective ultrasonic treatment ratio of 50%, a flow rate of 0.2 mL/min and a concentration of 0.043 M, with an applied power of 11 W (t_r = 80 s).

Frequency (kHz)	Dv(10) (μm)	Dv(50) (μm)	Dv(90) (μm)	Dv(90) – Dv(10) (μm)
21	2.63 ± 0.97	6.06 ± 4.19	18.4 ± 14.6	15.8 ± 13.7
46	1.94 ± 0.32	6.37 ± 1.22	16.4 ± 4.44	14.5 ± 4.17

Table 4
Effect of load power on the characteristic dimensions Dv(X) of the volume based PSD obtained at an effective ultrasonic treatment ratio of 50%, a flow rate of 0.2 mL/min and a concentration of 0.043 M, with an applied frequency of 21 kHz (t_r = 80 s).

Load power (W)	Dv(10) (μm)	Dv(50) (μm)	Dv(90) (μm)	Dv(90) – Dv(10) (μm)
11	2.63 ± 0.97	6.06 ± 4.19	18.4 ± 14.6	15.8 ± 13.7
22	2.31 ± 0.49	4.36 ± 1.94	8.01 ± 7.62	5.70 ± 7.14

3.4. Temperature profiles

One of the main drawbacks of using low frequency ultrasound is the associated temperature increase [8,18]. This temperature increase can have an impact on different scales. For chemical reactions, it is important to have an accurate temperature control, especially when working with temperature sensitive reactants, as it can impact the quality and yield of the reaction. This increase in temperature can also affect the gas solubility and vapor pressure, which will reduce the cavitation activity [9]. To quantify the effect of the different ultrasound conditions, the temperature in the reactor channel was recorded for a time equaling 5 reactor volumes at a flow rate of 0.2 mL/min, with an applied frequency of 21 kHz at a load power of 11 W.

Fig. 5 depicts the temperature profiles where the continuous line corresponds to continuous sonication and dashed lines to pulsed ultrasound conditions. It is observed that for continuous sonication the temperature continuously increases over the recording period and reaches 7 °C after 5 reactor volumes. Switching to pulsed ultrasound allows to decrease the temperature of the reaction mixture during the silent time. Thus, the overall temperature increase is reduced to 4 °C for 50% effective ultrasonic treatment ratio and to less than 1 °C for both conditions at 12.5% effective ultrasonic treatment ratio after 5 reactor volumes. For the 50% effective ultrasonic treatment ratio, the temperature of the reaction mixture at the end of each cycle is not the same as the one at the beginning of the ultrasonic cycle. This means that the micro-reactor transducer assembly needs more than 40 s to reach the initial temperature. This increase of temperature, if not controlled can have an impact on the aging of the piezoelectric materials. This aging of the piezoelectric element is related to the Curie temperature, which corresponds to the temperature at which a change in the magnetic properties of the materials occur [42]. The value of the slope at the origin of each curve is similar, which highlights that the same load power is delivered for each condition at different effective ultrasonic treatment ratios. This proves that the same amount of energy is transferred to the reaction mixture for each pulsed ultrasound condition

The same study was also performed at a load power of 23 W, where it is observed that the temperature increase after 5 reactor volumes scales with the applied load power. This increase is expected as the cavitation activity increases with load power. Quantifying the calorimetric power reveals that it increases from 0.18 W (11 W load power) to 0.36 W (23 W load power), and that the calorimetric power was the same for each effective ultrasonic treatment ratio condition. In conclusion, the temperature profiles clearly show that applying pulsed ultrasound minimizes the associated temperature increase while still preventing clogging. For the pulsed ultrasound conditions, it can be noticed that temperature increases at the start of each sonication sequence. This can allow to reactivate the cavitation activity.

4. Conclusions

The use of pulsed ultrasound conditions as a less invasive methods to prevent clogging in micro-channels for the synthesis of inorganic particles has been successfully investigated in this article. Experiments showed that applying a effective ultrasonic treatment ratio of 12.5% allowed to achieve this goal. It has been shown that both

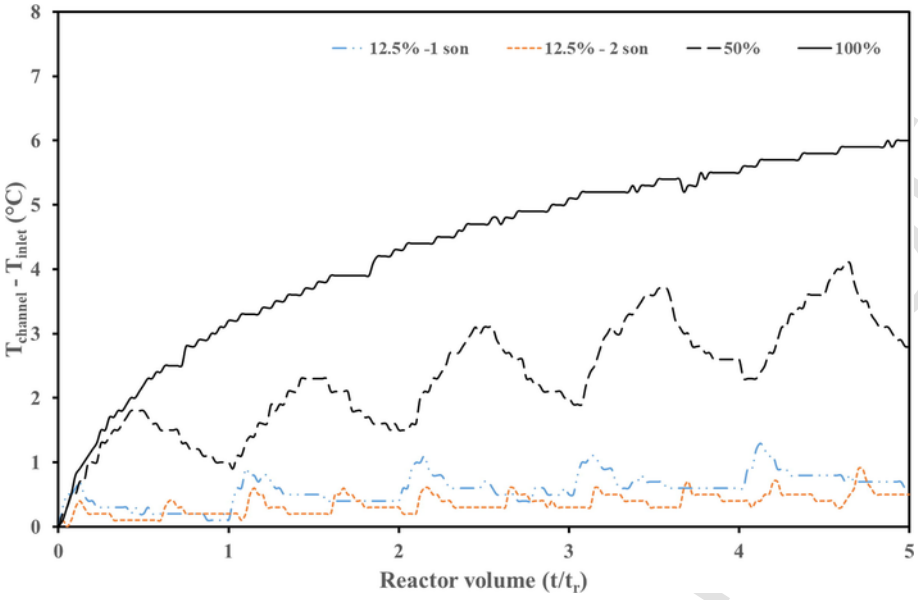

Fig. 5. Influence of effective ultrasonic treatment ratio on temperature profiles recorded for a time equaling 5 reactor volumes at a flow rate of 0.2 mL/min, with an applied frequency of 21 kHz at a load power of 11 W (t_r = 80 s). Studied effective ultrasonic treatment ratio corresponds to 12.5, 50 and 100%. Concerning the 12.5% of effective ultrasonic treatment ratio the cases with 1 and 2 pulses per reactor volume is studied.

pulsed and continuous sonication prevents clogging by breaking particle agglomerates, which lead to smaller mean particle size and a narrower size distribution. The mean size of barium sulfate particles was reduced from 20 μm under silent conditions to less than 6 μm depending on the ultrasonic parameters. The study of the number of pulses at a given effective ultrasonic treatment ratio showed that ultrasound allowed to break agglomerates formed during the growth time. Moreover, pulsed ultrasound has been successfully implemented to control the temperature of the reaction mixture. The temperature increase was reduced from 7 °C under continuous sonication to less than 1 °C at a duty cycle of 12.5%. Thus, combining pulsed ultrasound with micro-reactors enables to expand the applicability of these technologies in the chemical field.

Acknowledgments

This project has received funding from the European Union's Horizon 2020 research and innovation program under the Marie Sklodowska-Curie grant agreement No 721290. This publication reflects only the author's view exempting the Community from any liability. Project website: http://cosmic-etn.eu/. We thank Dr. Zhengya Dong for the design and the assembly of the ultrasonic micro-reactor.

References

[1] E.V. Kondratenko, Modern heterogeneous catalysis. an introduction By Rutger van Santen, Angew. Chemie Int. Ed. (2017) https://doi.org/10.1002/anie.201709088, pp. 13182–13182.

[2] D. Peters, Ultrasound in materials chemistry, J. Mater. Chem. 6 (1996) 1605–1618.

[3] J. Jordens, N. De Coker, B. Gielen, T. Van Gerven, L. Braeken, Ultrasound precipitation of manganese carbonate: the effect of power and frequency on particle properties, Ultrason. Sonochem. 26 (2015) 64–72, https://doi.org/10.1016/j.ultsonch.2015.01.017.

[4] J. Lee, M. Ashokkumar, S.E. Kentish, Influence of mixing and ultrasound frequency on antisolvent crystallisation of sodium chloride, Ultrason. Sonochem. 21 (2014) 60–68, https://doi.org/10.1016/j.ultsonch.2013.07.005.

[5] M.D. Luque de Castro, F. Priego-Capote, Ultrasound-assisted crystallization (sonocrystallization), Ultrason. Sonochem. 14 (2007) 717–724, https://doi.org/10.1016/j.ultsonch.2006.12.004.

[6] B. Pohl, R. Jamshidi, G. Brenner, U.A. Peuker, Experimental study of continuous ultrasonic reactors for mixing and precipitation of nanoparticles, Chem. Eng. Sci. 69 (2012) 365–372, https://doi.org/10.1016/j.ces.2011.10.058.

[7] J.A. Dodds, F. Espitalier, O. Louisnard, R. Grossier, R. David, M. Hassoun, F. Baillon, C. Gatumel, The effect of ultrasound on crystallisation-precipitation processes: some examples and a new segregation model, Part. Part. Syst. Charact. 24 (2007) 18–28.

[8] J.J. John, S. Kuhn, L. Braeken, T. Van Gerven, Temperature controlled interval contact design for ultrasound assisted liquid–liquid extraction, Chem. Eng. Res. Des. 125 (2017) 146–155, https://doi.org/10.1016/j.cherd.2017.06.025.

[9] Q.-A. Zhang, Y.-Y. Yan, X.-H. Fan, X.-L. Zhang, Effects of ultrasound working parameters on the ultrasonic power density some neglected problems in the application of ultrasound bath, Iran. J. Chem. Chem. Eng. 36 (2017) 161–171.

[10] T.J. Mason, Ultrasonic cleaning: an historical perspective, Ultrason. Sonochem. 29 (2016) 519–523, https://doi.org/10.1016/j.ultsonch.2015.05.004.

[11] E. Loranger, M. Paquin, C. Daneault, B. Chabot, Comparative study of sonochemical effects in an ultrasonic bath and in a large-scale flow-through sonoreactor, Chem. Eng. J. 178 (2011) 359–365, https://doi.org/10.1016/j.cej.2011.10.021.

[12] S.V. Dalvi, M.D. Yadav, Effect of ultrasound and stabilizers on nucleation kinetics of curcumin during liquid antisolvent precipitation, Ultrason. Sonochem. 24 (2015) 114–122, https://doi.org/10.1016/j.ultsonch.2014.11.016.

[13] J.J. John, S. Kuhn, L. Braeken, T. Van Gerven, Ultrasound assisted liquid-liquid extraction in microchannels-a direct contact method, Chem. Eng. Process. Process Intensif. 102 (2016) 37–46, https://doi.org/10.1016/j.cep.2016.01.003.

[14] J.J. John, S. Kuhn, L. Braeken, T. Van Gerven, Ultrasound assisted liquid–liquid extraction with a novel interval-contact reactor, Chem. Eng. Process. Process Intensif. 113 (2017) 35–41, https://doi.org/10.1016/j.cep.2016.09.008.

[15] O. Louisnard, F. Espitalier, Sono-crystallization : from experimental results to microscopical interpretations, 19th Int. Congr. Acoust., Madrid, 2007.

[16] B. Gielen, P. Kusters, J. Jordens, L.C.J. Thomassen, T. Van Gerven, L. Braeken, Energy efficient crystallization of paracetamol using pulsed ultrasound, Chem. Eng. Process. Process Intensif. 114 (2017) 55–66, https://doi.org/10.1016/j.cep.2017.01.001.

[17] Z. Guo, M. Zhang, H. Li, J. Wang, E. Kougoulos, Effect of ultrasound on anti-solvent crystallization process, J. Cryst. Growth 273 (2005) 555–563, https://doi.org/10.1016/j.jcrysgro.2004.09.049.

[18] F. Rahmani, M. Haghighi, S. Mahboob, CO2-enhanced dehydrogenation of ethane over sonochemically synthesized Cr/clinoptilolite-ZrO2nanocatalyst: effects of ultrasound irradiation and ZrO2loading on catalytic activity and stability, Ultrason. Sonochem. 33 (2016) 150–163, https://doi.org/10.1016/j.ultsonch.2016.04.034.

[19] D.C. Boffito, V. Crocellà, C. Pirola, B. Neppolian, G. Cerrato, M. Ashokkumar, C.L. Bianchi, Ultrasonic enhancement of the acidity, surface area and free fatty acids esterification catalytic activity of sulphated ZrO2-TiO2 systems, J. Catal. 297 (2013) 17–26, https://doi.org/10.1016/j.jcat.2012.09.013.

[20] L. Jiang, A. Wang, Y. Zhao, J. Zhang, J. Zhu, A novel route for the preparation of monodisperse silver nanoparticles via a pulsed sonoelectrochemical technique, Inorg. Chem. Commun. 7 (2004) 506–509, https://doi.org/10.1016/j.inoche.2004.02.003.

[21] J. Zhu, Z. Lu, S.T. Aruna, D. Aurbach, A. Gedanken, Sonochemical synthesis of SnO2nanoparticles and their preliminary study as Li insertion electrodes, Chem. Mater. (2000) https://doi.org/10.1021/cm990683l.

[22] I. Haas, S. Shanmugam, A. Gedanken, Pulsed sonoelectrochemical synthesis of size-controlled copper nanoparticles stabilized by poly (N-vinylpyrrolidone), J. Phys. Chem. B 110 (2006) 16947–16952, https://doi.org/10.1021/jp064216k.

[23] M. Ashokkumar, The characterization of acoustic cavitation bubbles – an overview, Ultrason. Sonochem. 18 (2011) 864–872, https://doi.org/10.1016/j.ultsonch.2010.11.016.
[24] V. Ciaravino, H.G. Flynn, M.W. Miller, Pulsed enhancement of acoustic cavitation: a postulated model, Ultrasound Med. Biol. 7 (1981) 159–166, https://doi.org/10.1016/0301-5629(81)90005-3.
[25] J. Zhu, S. Liu, O. Palchik, Y. Koltypin, A. Gedanken, Shape-controlled synthesis of silver nanoparticles by pulse sonoelectrochemical methods, Langmuir (2000) 6396–6399, https://doi.org/10.1021/la991507u.
[26] R.L. Hartman, K.F. Jensen, Microchemical systems for continuous-flow synthesis, Lab Chip 9 (2009) 2495–2507, https://doi.org/10.1039/b906343a.
[27] J.I. Yoshida, H. Kim, A. Nagaki, Green and sustainable chemical synthesis using flow microreactors, ChemSusChem 4 (2011) 331–340, https://doi.org/10.1002/cssc.201000271.
[28] K.S. Elvira, X.C.I. Solvas, R.C.R. Wootton, A.J. Demello, The past, present and potential for microfluidic reactor technology in chemical synthesis, Nat. Chem. 5 (2013) 905–915, https://doi.org/10.1038/nchem.1753.
[29] D. Fernandez Rivas, S. Kuhn, Synergy of microfluidics and ultrasound: process intensification challenges and opportunities, Top. Curr. Chem. 374 (2016) https://doi.org/10.1007/s41061-016-0070-y.
[30] S. Kuhn, T. Noël, L. Gu, P.L. Heider, K.F. Jensen, A Teflon microreactor with integrated piezoelectric actuator to handle solid forming reactions, Lab Chip 11 (2011) 2488–2492, https://doi.org/10.1039/c1lc20337a.
[31] R.L. Hartman, J.R. Naber, N. Zaborenko, S.L. Buchwald, K.F. Jensen, Overcoming the challenges of solid bridging and constriction during Pd-catalyzed C-N bond formation in microreactors, Org. Process Res. Dev. 14 (2010) 1347–1357, https://doi.org/10.1021/op100154d.
[32] T. Noël, J.R. Naber, R.L. Hartman, J.P. McMullen, K.F. Jensen, S.L. Buchwald, Palladium-catalyzed amination reactions in flow: overcoming the challenges of clogging via acoustic irradiation, Chem. Sci. 2 (2011) 287–290, https://doi.org/10.1039/C0SC00524J.
[33] Z. Dong, D. Fernandez Rivas, S. Kuhn, Acoustophoretic focusing effects on particle synthesis and clogging in microreactors, Lab Chip 19 (2019) 316–327, 10.1039/c8lc00675j.
[34] Z. Dong, C. Yao, X. Zhang, J. Xu, G. Chen, Y. Zhao, Q. Yuan, A high-power ultrasonic microreactor and its application in gas–liquid mass transfer intensification, Lab Chip 15 (2015) 1145–1152, https://doi.org/10.1039/c4lc01431f.
[35] S. Zhao, Z. Dong, C. Yao, Z. Wen, G. Chen, Q. Yuan, Liquid-liquid two-phase flow in ultrasonic microreactors: cavitation, emulsification, and mass transfer enhancement, AIChE J. 00 (2017) 1–12, https://doi.org/10.1002/aic.16010.
[36] Z. Dong, C. Yao, Y. Zhang, G. Chen, Q. Yuan, J. Xu, Hydrodynamics and mass transfer of oscillating gas-liquid flow in ultrasonic microreactors, AIChE J. 62 (2016) 1294–1307, https://doi.org/10.1002/aic.15091.
[37] P.R. Gogate, V.S. Sutkar, A.B. Pandit, Sonochemical reactors: important design and scale up considerations with a special emphasis on heterogeneous systems, Chem. Eng. J. 166 (2011) 1066–1082, https://doi.org/10.1016/j.cej.2010.11.069.
[38] F. Castro, S. Kuhn, K. Jensen, A. Ferreira, F. Rocha, A. Vicente, J.A. Teixeira, Continuous-flow precipitation of hydroxyapatite in ultrasonic microsystems, Chem. Eng. J. 215–216 (2013) 979–987, https://doi.org/10.1016/j.cej.2012.11.014.
[39] J. Baldyga, M. Jasińska, W. Orciuch, Barium sulphate agglomeration in a pipe – an experimental study and CFD modeling, Chem. Eng. Technol. 26 (2003) 334–340, https://doi.org/10.1002/ceat.200390051.
[40] D. Marchisio, A. Barresi, M. Garbero, M. Vanni, G. Baldi, Study of aggregation in barium sulphate precipitation, 15th Int. Symp. Ind. Cryst., 2002.
[41] Z. Guo, A.G. Jones, N. Li, Interpretation of the ultrasonic effect on induction time during BaSO4 homogeneous nucleation by a cluster coagulation model, J. Colloid Interface Sci. 297 (2006) 190–198, https://doi.org/10.1016/j.jcis.2005.10.035.
[42] L. Hallez, Caractérisation de transducteurs ultrasonores focalisés (HIFU) dédiés à la sonochimie: application à l'irradiation de polymères, Université de Franche-Comté (2009).